Optical Fish Estimation and Detection in Noisy Environment

Mohcine Boudhane*,†, Sabah Badri-Hoeher*, and Benayad Nsiri†
*Faculty of Computer Science and Electrical Engineering, University of Applied Sciences, Grenzstr. 5, 24149 Kiel, Germany
†University Hassan II, Faculty of Sciences, Ainchock B.P 5366 Maarif 20000, Casablanca, Morocco
Email: {mohcine.boudhane, sabah.badri-hoeher}@fh-kiel.de, benayad.nsiri@enst-bretagne.fr

***Abstract*—Detecting fish in submarine environment is a challenge due to the properties of the water such as light absorption and scattering. In this work, we present a method for pre-processing images in submarine environment. In the first step, we model the underwater environment as overlapp of two processes. The first process is considered as a Poisson distribution, while the second one is considered as a Gaussian mixture. The resulting distribution is called Poisson-Gaussian mixture (PGM). To estimate the noise parameters, we propose an iterative algorithm based on the expectation maximization approach. This allows us to jointly estimate the scale of the Poisson parameter as well as the standard deviation and the mean of all Gaussian distributions. In order to facilitate the detection of objects, to correct the illumination problem of the scene and to restore the colors, we integrate a color correction algorithm. Finally, detection and localization of fish complete the pre-processing in the images. To obtain medium or small regions, the mean shift algorithm is used with a reduced threshold. In the segmentation process, the proposed detector scan the image region by region. This detector allows to estimate statistically the type of the region (object or non-object). The method is tested under different underwater conditions. Experimental results show that the proposed approach outperforms conventional methods.**

I. Introduction

The field of detection in the marine environment is a hot topic since many years, due to the properties of under water and the limitation of human access in this environment. Many technologies have been developed to monitor and track the evolution of the marine environment such as remotely operated vehicles (ROVs), system targeting objects (STOs), and autonomous underwater vehicles (AUVs) [1], [2], [3].

Today, most underwater detection and monitoring systems are based on cameras and the exploitation of the image data. Computer vision and image processing have been particularly studied in this context to develop robust and sophisticated algorithms for underwater research topics. The light absorption and scattering pose a bottleneck, because the underwater visibility is only a few meters. In [4], where clear water is considered, twenty meters visibility is shown.
Recent works try to enhance the underwater image quality, and to reduce the level of noise in order to successfully detect and localize objects. Some researchers in [5], [6], [7] propose filter-based methods for reduction of undesirable noise. In [8] and [9] wavelet-based methods are proposed. In [8], the authors combine wavelet decomposition and high-pass filtering in order to remove back-scattering noise. Homomorphic filtering, anisotropic filtering and wavelet-based thresholding are applied to reduce the additive noise in [9]. However, these wavelet based methods cause unsharpness in the resulting image. In [10], the authors use a median filter to remove the noise, RGB color level stretching to enhance the quality of the image, and dark channel prior to obtain the atmospheric light. This method can only help in the case of images with minor noise. Very noisy images were treated in [11] by utilizing a bilateral filtering. The proposed solution presents good result but the required processing time is high.

Statistical methods are proposed in [12], [13], [14]. These methods are based on the modulation of noise as Poisson-Gaussian distribution and supposing that the image is independent from the noise. The authors show promising results at different noise levels.

Besides noise, the absorption, and scattering of light between the camera and the object, degrade the quality of captured images. The non-uniform absorption of colors, for example, red color is absorbed more than blue color, that make the underwater images dominated by the blue color. This behavior enhances the difficulties of identification and detection of divers, fish and other objects in underwater images. [15], [16], [17] apply regularization methods by means of laser technologies. Color polarization methods are proposed in [18], [19], [20]. The authors utilize a filter (at the front of the camera) in order to make the color proportions uniform in captured images. The combination of the laser based technology and color polarization are proposed in [21], [22].

The challenge now is to create an efficient tool which is able to solve jointly the problem of noise, light absorption, and scattering effects. Our goal is to offer the submarine biologists a tool to explore the underwater environment and analyze the behavior of different fish species. Several additional effects such as rain, whirlpool, current, salinity, temperature, waves, tides, and many other effects make the visibility more difficult (see Fig. 1). Fig. 2 defines the skills of our approach. It is divided on four fundamental blocks: image denoising, enhancement, segmentation, and detection in order to generalize the image pre-processing solution without knowledge of the environment.

The next sections in this paper are organized as follows. Section II describes the theoretical principle of the model under investigation. In this part, the denoising-enhancement process as well as statistical estimation of the desired object are derived. In Section III, experimental results and comparison with other methods are shown. Section IV concludes this work.

978-1-4799-4918-2/14/$31.00 ©2014 IEEE

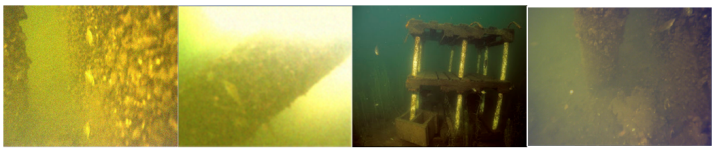

Figure 1. Examples of image scenes.

II. Theoretical Principle

The goal of the proposed approach is to extremely reduce the noise level in order to enhance the quality of the images in the submarine environment. There are principally two sources of noise: The first one is coming from the capture. It usually depends on the capture settings and the power of the device. The second is caused in the transmission, a typical example is the information loss due to image compression. Otherwise, without compression we would have to consume several temporal and material resources for the transmission of images (Fig. 3).

The Gaussian mixture is among the most popular models applied in statistics [23], [24]. It is a parametric probability density function represented as a weighted sum of Gaussian component densities. A Gaussian mixture model is a weighted sum of M component Gaussian densities as given by the equation, The Gaussian mixture is among the most popular models applied in statistics [23], [24]. It is a parametric probability density function represented as a weighted sum of Gaussian component densities. A Gaussian mixture model is a weighted sum of m component Gaussian densities as given by the equation, The Gaussian mixture is among the most popular models applied in statistics [23], [24]. It is a parametric probability density function represented as a weighted sum of Gaussian component densities. A Gaussian mixture model is a weighted sum of m component Gaussian densities as given by

$$p(\mathbf{y}) = \sum_{m=1}^{M} \alpha_m \cdot f(\mathbf{y}, \mathbf{C}_m, \boldsymbol{\mu}_m), \tag{1}$$

where each component density is defined as

$$f(\mathbf{y}) = \frac{1}{\sqrt{2\pi} \mid \mathbf{C}_m \mid^{\frac{1}{2}}} \exp\left\{-\frac{1}{2}(\mathbf{y}-\boldsymbol{\mu}_m)^T \mathbf{C}_m^{-1}(\mathbf{y}-\boldsymbol{\mu}_m)\right\}, \tag{2}$$

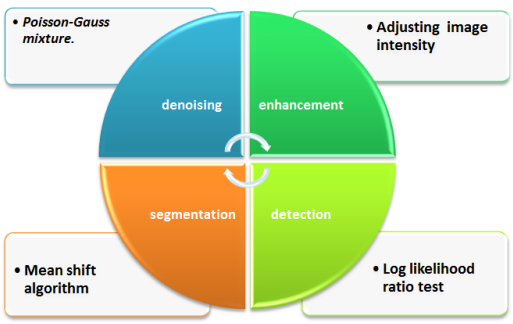

Figure 2. Skills of the proposed approach.

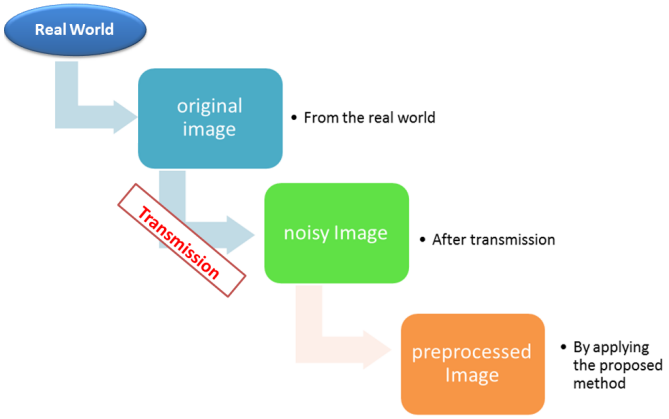

Figure 3. Sources of noise.

where $\mathbf{y}$ is a data vector, $\boldsymbol{\mu_m}$ is the mean vector, $\mathbf{C}_m$ is the covariance matrix, α_m are the mixture weights $(1 \leq m \leq M)$, where the mixture weights satisfy the constraint

$$\sum_{m=1}^{M} \alpha_m = 1. \tag{3}$$

In [25] the authors create a statistical model based on a mixture of projected Gaussian distribution and wavelet based algorithms, in which they use the expectation maximization algorithm to accelerate the processing time of the algorithm. This method implicitly segments the image into regions of similar content.
Poisson-Gaussian distribution is a statistical model formed by the combination of a Poisson distribution and a Gaussian distribution. In [12] the authors show that the noise produced in the imaging devices can be modeled as Poisson-Gaussian distribution. This combination generates a method of noise removal. The aim of the method is to benefit from the property of each distribution in image denoising. The Poisson component accounts for the signal-dependent uncertainty, while the Gaussian mixture component accounts for the other signal-independent noise sources. The Poisson-Gaussian can use generalized Anscombe transform to stabilize the variance [12], and to ensure the precision of the denoising process. The authors use this technique to treat pictures with low intensity.

In order to improve the perception of underwater images, we propose a new approach based on Poisson-Gaussian model. We assume that the mean and the variance of the noise are not constant in the whole image. By means of the Poisson-Gaussian mixture, the denoising process is adapted to each region in the image. Furthermore, each Gaussian in the mixture takes a set of pixels (e.g. background or foreground pixels), which gives additional information to the next step of the processing.

Let X be a random process that follows a Poisson distribution with parameter $x > 0$, then the probability mass function of X is given by

$$p_X(x) = \frac{e^{-x}x^k}{k!}, \tag{4}$$

and let Y be a random variable that follows a Gaussian distribution with variance σ^2 and mean μ, then the probability density function is given by

$$p_Y(y) = \frac{1}{\sqrt{2\pi\sigma^2}} e^{\frac{-(y-\mu)^2}{2\sigma^2}}, \tag{5}$$

where x and y are the realizations of the random variable X and Y, respectively.
Let $Z = (Z_1, Z_2, \cdots, Z_N)$ be a series of observations that form a set of random independent variables, and z_n be realizations of Z that are considered to be the measure of noise intensity of the signal I. From [12], the Poisson-Gaussian distribution is defined by

$$p(z|y,\sigma) = \sum_{k=0}^{\infty} \frac{x^k}{k!} e^{-x} \frac{1}{\sqrt{2\pi\sigma^2}} e^{\frac{-(z-k)^2}{2\sigma^2}}. \tag{6}$$

The idea of this work is to generalize the Poisson-Gaussian distribution by means of several Gaussian. This new distribution is called Poisson-Gaussian Mixture distribution (PGM). It is defined as

$$p(z|\mathbf{y}) = \sum_{k=0}^{\infty} \left(\frac{x^k}{k!} e^{-x} \sum_{m=1}^{M} \alpha_m \cdot f(\mathbf{y}, \mathbf{C}_m, \boldsymbol{\mu}_m) \right), \tag{7}$$

where x is a strictly positive real number, M is the number of Gaussians, $\mathbf{C}_m$ is the covariance matrix of the m^{th} Gaussian, and $\boldsymbol{\mu}_m$ and α_m are the m^{th} mean and mixture coefficient, respectively.

A. Estimation of the image parameters

The estimation of the parameters $(\alpha_m, \boldsymbol{\mu}_m, \mathbf{C}_m)$ will be done by means of the expectation maximization algorithm (EM). The estimation can also be done by means of the maximum likelihood estimation algorithm [26]. Given training vectors and a Poisson-Gaussian mixture configuration, the goal is to estimate the parameters $(\alpha_m, \boldsymbol{\mu}_m, \mathbf{C}_m)$ of this distribution, that best match the distribution of the training feature vectors.

The aim of the EM-algorithm is to maximize the likelihood function with respect to the parameters under investigation. This estimation can be divided into four steps:

1. Initialization step: $\boldsymbol{\mu}_m$, $\mathbf{C}_m$, α_m and log-likelihood are initialized.

2. Expectation step: Evaluation of the posterior probabilities using the current parameter values:

$$\gamma(z_{nm}) = \frac{\alpha_m p(\mathbf{x}_n|\boldsymbol{\mu}_m, \mathbf{C}_m)}{\sum_{j=1}^{M} \alpha_j p(\mathbf{x}_n|\boldsymbol{\mu}_j, \mathbf{C}_j)}, \tag{8}$$

where $\gamma(z_{nm})$ defines the posterior probabilities for the n^{th} observation, and M is the total number of Gaussians in the mixture.

3. Maximization step: Computation of the parameters using the current posterior probabilities

$$\alpha_m{}^{new} = \frac{N_m}{N}, \tag{9}$$

$$\boldsymbol{\mu}_m^{new} = \frac{1}{N_m} \sum_{n=1}^{N} \gamma(z_{nm}) \mathbf{x}_n, \tag{10}$$

$$\mathbf{C}_m^{new} = \frac{1}{N_i} \sum_{n=1}^{N} \gamma(z_{nm}) (\mathbf{x}_n - \boldsymbol{\mu}_m^{new})(\mathbf{x}_n - \boldsymbol{\mu}_m^{new})^T, \tag{11}$$

where N_m denotes the effective number of pixels assigned to the cluster m, where

$$N_m = \sum_{n=1}^{N} \gamma(z_{nm})$$

.

4. Evaluation step: Evaluation of the log-likelihood function:

$$\ln(p(\mathbf{x}|\mathbf{y})) = \sum_{n=1}^{N} \ln \left(\sum_{m=1}^{M} \alpha_m p(\mathbf{x}_n|\boldsymbol{\mu}_m, \mathbf{C}_m) \right), \tag{12}$$

where M is the total number of Gaussians.
The last iteration of the algorithm is achieved when the log-likelihood function and the parameters converge to a constant value.

Finally the resulting filter model will be convolved with the original image, in order to reduce the noise.

B. Segmentation

Several methods have been developed for segmenting images. The choice of an adequate technique depends on many factors (segmentation of medical images is different from underwater images). In this work, we chose to use the so-called mean-shift algorithm in the segmentation.
The mean-shift algorithm was introduced by Fukunaga and Hostetler in [27], and has been extended to be applicable in other fields like computer vision [28]. It is a powerful non-parametric iterative algorithm that can be used for many purposes (segmentation, clustering,$\cdots$). Mean-shift associates segments with the nearby pixels of the dataset probability density function. For each segment, mean-shift defines a window around it and computes the mean of the data points, then it shifts the center of the window to the mean and repeats the algorithm until it converges. After each iteration, the window shifts to a denser region of the image.

At the highest level, the mean-shift algorithm is specified as follows:

1. Fix a window around each data point.
2. Compute the mean of data within the window.
3. Shift the window to the mean, and repeat until the algorithm converges.

In this phase, we obtain the segmented image that include several regions (see Fig. 4). Each region is isolated, and then treated separately in order to make a statistical test on it.

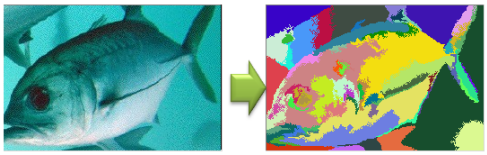

Figure 4. Image segmentation via the mean-shift algorithm.

Fig. 5 shows this isolation applied on the segmented image. In the remainder of this section, the log-likelihood ratio test is carried out in order to measure the reliability of the estimation that the object exists. Then, the obtained value is verified and compared with the original data.

C. The log-likelihood ratio test

The likelihood ratio method expresses how many times a test result is likely to be found in true compared with false hypothesis. This method always gives a feasible equation, and it can be used when we have truncated data. The likelihood ratio (LR) is written by

$$\mathrm{LR} = \frac{P(Test_{\text{true}})}{P(Test_{\text{false}})}. \tag{13}$$

Let $\mathbf{s} = [s_1, \cdots s_N]^T$ denote regions of a given image. We suppose these regions follow a Poisson-Gaussian mixture distribution, furthermore we assume that the segments are statistically independent. With this assumption, the proposed method takes the following forms as a log-likelihood ratio test:

$$\mathrm{LLR} = \frac{p(\mathbf{s}|H_0)}{p(\mathbf{s}|H_1)}, \tag{14}$$

where H_0 and H_1 be two hypotheses. H_0 is the hypothesis of existing object, and H_1 of non-existing one.

In the case of color images, the result is the addition of each LLR associated to each color component. For example, in the RGB space, it is recommended to use the following equation:

$$\mathrm{LLR} = \mathrm{LLR}_{Red} + \mathrm{LLR}_{Green} + \mathrm{LLR}_{Blue}$$

III. Experimental results:

In this section, the proposed approach is compared with conventional methods. The system is implemented on a standard PC. Different images of different sizes have been used in the experiment.

Figure 5. Image decomposition via the mean shift algorithm

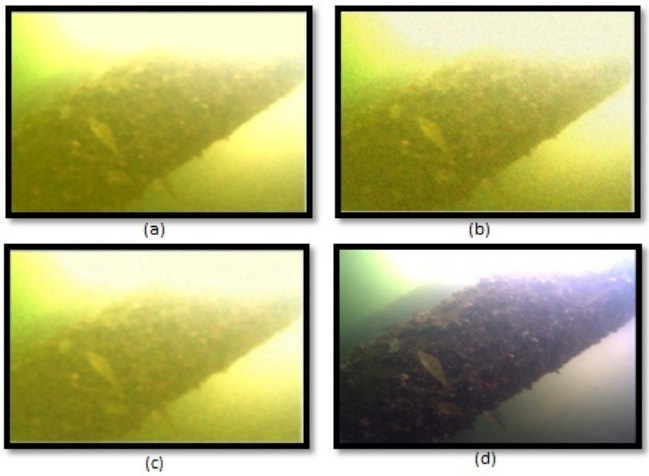

Figure 6. Denoising process for our approach: (a) Original image, (b) Noisy image, (c) Denoised with the proposed approach, (d) Correction by means of color filtering.

Fig. 6 shows the different steps of pre-processing images. Fig. 6b is corrupted with additive Gaussian white noise at eight different power levels $\sigma = 15$dB. Fig. 6c and Fig. 6d show the denoised and enhanced image respectively. In Fig. 6d, we obtained a more clear image than the original image. The numerical results for different levels of noise is shown in the Tables I and II.

Fig. 7 represents the results of estimation by log-likelihood ratio test. It shows the objects estimated in the image. In Fig. 7a several small regions are obtained, that include the estimated objects. After thresholding, the number of false regions is reduced, then we obtain the new estimation of the object (see Fig. 7b).

Before presenting the results, we review some terminologies, which will be used in the following numerical analysis. Mean squared error (MSE) and pixel signal-to-noise ratio (PSNR) are used to determine the reconstructed image quality. MSE is defined by the following equation

$$\mathrm{MSE} = \frac{\sum_{j=1}^{H}\left(\sum_{i=1}^{W}(S_{i,j} - S^r_{i,j})^2\right)}{HW}, \tag{15}$$

where $S_{i,j}$ and $S^r_{i,j}$ represent pixels of the original and the reconstructed (HxW) image, respectively. *The pixel signal to noise ratio* ($PSNR$) (in dB) is calculated using the following equation:

$$\mathrm{PSNR} = 10 \cdot \log\left\{\frac{(255)^2}{\mathrm{MSE}}\right\}. \tag{16}$$

The proposed approach is tested in different images. Table I and II present the PSNR value for each denoising method, and thereafter, we resume these results in Fig. 8.

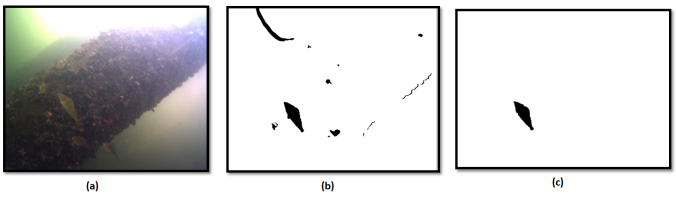

Figure 7. Segmentation and fish estimation process: (a) Enhanced image (b) Automatic segmentation and statistical estimation (c) Segmentation and statistical estimation with threshold regularization.

Table I. PSNR FOR TEST IMAGES UNDER INVESTIGATION

$\sigma/PSNR(input)$	PSNR (output, proposed approach)
5 / 34.55	34.82
10 / 28.34	30.99
15 / 24.92	29.31
20 / 22.53	28.23
30 / 19.20	26.71
50 / 15.19	24.31

Table I and II present the PSNR value calculated by the proposed approach after the denoising process. Each line is corrupted with additive Gaussian white noise at six different noise levels ($\sigma = \{5, 10, 15, 20, 30, 50\}$). Different algorithms are applied to the same noise realizations.

Table II. COMPARISON OF FILTER OUTPUT PSNR USING THE FIRST IMAGE (FISH)

σ	Gaussian Filter	Median Filter	Bilateral Filter	NLM Filter[1]
5	25.91	27.75	33.57	32.69
10	25.85	27.25	32.05	29.50
15	25.76	26.54	29.38	28.34
20	25.61	25.72	26.23	27.62
30	25.17	24.07	21.18	26.38
50	23.77	21.17	15.79	23.79

The graph in Fig. 8 shows the output PSNR values comparing with different levels of noise throughout pre-processing by median filter, bilateral filter and the proposed approach. The output PSNR values of the proposed approach are relatively higher at values of σ less than 15 comparing with median filter. We can see that the Bilateral Filter and our approach has an output PSNR more than 30 dB. Also, we can see that between $\sigma = 8$ and $\sigma = 15$ bilateral filter has a small advantage over our method. However, from $\sigma = 15$ the percentage declined to a peak around 30 dB. and from $\sigma = 20$ the median filter offers more quality than bilateral filter. On the other hand, when we see all graphs, it declines gradually with respect to noise enhancement σ. From $\sigma = 15$ the output PSNR of the proposed approach is relatively higher than the other approaches. This implies that the greater is the noise, the less sensitive is our approach compared with conventional methods.

[1]non local mean filter

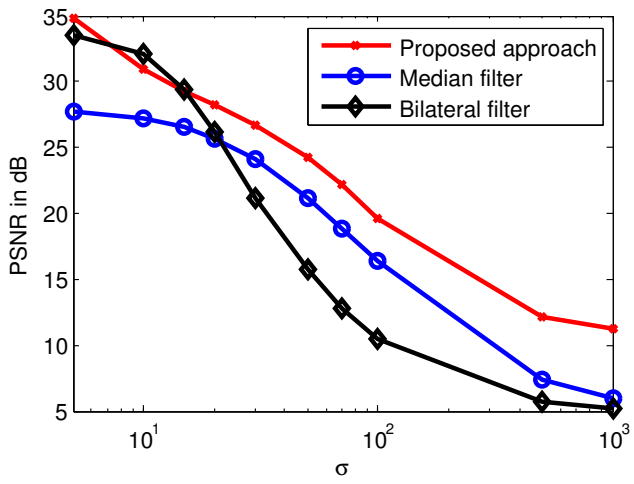

Figure 8. Performance comparison.

The log-likelihood ratio test results :

Table III. LLR TEST RESULTS

Case	Fig. 8a	Fig. 8d
Total regions	5	29
object regions	1	28
log-likelihood ratio	-334	403
decision	No	Yes

Table III illustrates the log-likelihood ratio before and after applying the pre-processing process. We can see in Table III that before the pre-processing, the log-likelihood ratio test value is unable to detect enough objects regions, in order to predict the existence of the object. The image input is noisy and the system rejects the possibility of the existence of the object in the image. However, after pre-processing, the system can detect more regions, that help the system to give the right decision. In conclusion, our approach has a good performance in terms of denoising and enhancement, which permit to the log-likelihood ratio test to make decisions by estimating the existence of objects.

IV. CONCLUSION

In this work, we have proposed a new method for underwater image pre-processing. Than we proposed a Poisson-Gaussian mixture distribution for the modulation and filtering of the noise. We strengthen the method by applying a statistical process based on the calculation of the log-likelihood ratio and their use as a test for detecting object or non-object in underwater images. The obtained results show that the proposed method outperforms conventional pre-processing methods.

REFERENCES

[1] S. Veerachart, P. Patompak, and N. Itthisek, "A robust adaptive control algorithm for remotely operated underwater vehicle," in *Proc. SICE '13*, Nagoya, Japan, 2013, pp. 655–660.

[2] D. Liang, Q. Huang, S. Jiang, H. Yao, and G. W., "Autonomic management for the next generation of autonomous underwater vehicles," in *Proc. IEEE ICIP '07*, Southampton, UK, 2007, pp. 369–372.

[3] W. Kirkwood, "AUV technology and application basics," in *Proc. MTS/IEEE OCEANS '08*, Kobe, Japan, 2008, p. 15.

[4] M. Legris, K. Lebart, F. Fohanno, and B. Zerr, *Les capteurs dimagerie en robotique sous-marine: tendances actuelles et futures*. Saint Martin d'Hres, France: GRETSI, 2003.

[5] C. Chang, J. Hsiao, and C. Hsieh, "An adaptive median filter for image denoising," in *Proc. IEEE IITA '08*, Qingdao, China, 2008, pp. 346–50.

[6] C. Wang and J. Zhang, "Image denoising via clustering-based sparse representation over Wiener and Gaussian filters," in *Proc. IEEE S-CET '12*, Qingdao, China, 2012, pp. 1–4.

[7] A. Nath, "Image denoising algorithms: A comparative study of different filtration approaches used in image restoration," in *Proc. IEEE CSNT '13*, Gwalior, India, 2013, pp. 157–163.

[8] P. Prabhakar and P. Kumar, "Underwater image denoising using adaptive wavelet subband thresholding," in *Proc. IEEE ICSIP '10*, Chennai, India, 2010, pp. 322–327.

[9] S. Feifei, Z. Xuemeng, and W. Guoyu, "An approach for underwater image denoising via wavelet decomposition and high-pass filter," in *Proc. IEEE ICICTA '11*, Shenzhen, China, 2011, pp. 417–420.

[10] M. Donna, F. Kocak, and M. Caimi, "The current art of underwater imaging - with a glimpse of the past and vision of the future," *Marine Technology Society Journal*, vol. 39, no. 3, pp. 5–26, 2005.

[11] M. Zhang and B. Gunturk, "Multiresolution bilateral filtering for image denoising," *IEEE Trans. Image Process.*, vol. 17, no. 12, pp. 2324–2333, Dec 2008.

[12] M. Makitalo and A. Foi, "A optimal inversion of the generalized Anscombe transformation for Poisson-Gaussian noise," *IEEE Trans. Image Processing*, vol. 22, no. 1, pp. 91–103, Jan 2013.

[13] A. Jezierska, E. Chouzenoux, J. Pesquet, and H. Talbot, "A primal-dual proximal splitting approach for restoring data corrupted with Poisson-Gaussian noise," *IEEE Trans. Image Processing*, vol. 22, no. 1, pp. 91–103, Jan 2014.

[14] A. Foi, "Noise estimation and removal in mr imaging: the variance-stabilization approach," in *Proc. IEEE Biomedical Imaging conference '11*, Chicago, USA, 2011, pp. 1809–1814.

[15] J. Forand, G. Fournier, D. Bonnier, and P. Pace, "Lucie: a laser underwater camera image enhancer," in *Proc. MTS/IEEE OCEANS '93*, Victoria, 1993, pp. 187–190.

[16] Y. Shubin and P. Fuyuan, "Laser underwater target detection based on Gabor transform," in *Proc. IEEE ICCSE '09*, Nanning, China, 2009, pp. 95–97.

[17] B. Ouyang, F. Dalgleish, A. Vuorenkoski, W. Britton, B. Ramos, and B. Metzger, "Visualization and image enhancement for multistatic underwater laser line scan system using image-based rendering," *IEEE journal of Oceanic Engineering*, vol. 38, no. 3, pp. 566–580, Jan 2013.

[18] L. Yongguo and S. Wang, "Underwater polarization imaging technology," in *Proc. CLEO/PACIFIC RIM '09*, Shanghai, China, 2009, pp. 1–2.

[19] V. Gruev, J. Van der Spiegel, and N. Engheta, "Advances in integrated polarization image sensors," in *Proc. IEEE/NIH LiSSA'09*, Bethesda, USA, 2009, pp. 62–65.

[20] P. Chang, J. Flitton, K. Hopcraft, E. Jakeman, D. Jordan, and J. G. Walker, "Improving visibility depth in passive underwater imaging by use of polarization," *IEEE journal of Oceanic Engineering*, vol. 42, no. 15, pp. 2794–2803, 2003.

[21] L. Jin, L. Gao, L. Huo, W. Yuan, Y. Luo, A. Ho, and C. Lin, "Technique for false image correction in second harmonic generation microscopy by modulating laser polarization," in *Proc. International Symposium Metamaterials'06*, Hangzhou, China, 2006, pp. 72–75.

[22] B. Swartz and D. James, "Laser range-gated underwater imaging including polarization discrimination," *SPIE*, vol. 42, no. 15, pp. 42–56, Dec 1991.

[23] S. Dasgupta, "Learning mixtures of Gaussians," in *Proc. IEEE SF-FCS'99*, New York, USA, 1999, pp. 634–644.

[24] M. Jordan, J. Kleinberg, and B. Scholkopf, *Information Science and Statistics*, 1st ed. Cambridge, U.K.: Springer, 2006.

[25] H. Rabbani, M. Vafadoost, and I. Selesnick, "Wavelet based image denoising with a mixture of Gaussian distributions with local parameters," in *Proc. ELMAR'06*, Zadar, Croatia, 2006, pp. 85–88.

[26] F. Liu, Y. Wang, P. Wang, and J. Huang, "Two iterative algorithms for maximum likelihood esitimation of Gaussian mixture parameter," in *Proc. IEEE ICNC'13*, Shenyang, China, 2013, pp. 1454–1458.

[27] K. Fukunaga and L. Hostetler, "The estimation of the gradient of a density function, with applications in pattern recognition," *IEEE Trans. Information Theory*, vol. 21, no. 1, pp. 32–40, 1975.

[28] D. Liang, Q. Huang, S. Jiang, H. Yao, and H. Gao, "Mean shift blob tracking with kernel histogram filtering and hypothesis testing," *ELSIVER, Pattern Recognition Letters*, vol. 26, no. 5, pp. 605–614, August 2004.